

Article

Effects of Reduced Ambient Pressure and Beam Oscillation on Gap Bridging Ability during Solid-State Laser Beam Welding

Markus Köhler *, Tamás Tóth, Andreas Kreybohm, Jonas Hensel  and Klaus Dilger

Institute for Joining and Welding, Technische Universität Braunschweig, Langer Kamp 8, 38106 Braunschweig, Germany; t.toth@tu-braunschweig.de (T.T.); a.kreybohm@tu-braunschweig.de (A.K.); j.hensel@tu-braunschweig.de (J.H.); k.dilger@tu-braunschweig.de (K.D.)

* Correspondence: markus.koehler@tu-braunschweig.de; Tel.: +49-531-391-95532

Received: 30 March 2020; Accepted: 27 April 2020; Published: 29 April 2020



Abstract: In recent decades, beam welding processes have been set up as a key technology for joining applications in automotive engineering and particularly in gearbox manufacturing. Due to their high beam quality, energy efficiency, reliability as well as flexible beam guidance, modern solid-state lasers offer numerous advantages, but also pose increased requirements on the production and positional accuracy of the components for the joining process. In particular, small-focus diameters present a challenge for components with process-induced tolerances, i.e., disc carriers in automatic transitions. Furthermore, welding processes utilizing solid-state lasers show an increased spatter formation during welding at high welding speeds. Accordingly, the primary objective of the presented work consists in extending the current areas of application for solid-state laser beam welding in gearbox manufacturing through an improved process reliability regarding tolerance compensation and spatter formation. Therefore, this experimental study aimed to describe the effects of a dynamic beam oscillation in combination with a reduced ambient pressure in the process environment on both gap bridging ability and spatter formation during the laser beam welding of case hardening steel. For basic process evaluations, laser beam welding at reduced ambient pressure and laser beam welding with dynamic beam oscillation were initially studied separately. Following a basic process evaluation, samples for 2 mm full-penetration-welds with varying gap sizes were analyzed in terms of weld seam geometry and weld spatter formation.

Keywords: laser welding; beam oscillation; reduced ambient pressure; gap bridging; case hardening steel; gearbox manufacturing

1. Introduction

The current trends in the automotive industry show an increased demand for the power beam technologies, particularly in the sheet metal processing as well as in powertrain manufacturing, induced by the continuous development in laser beam sources, optics and electronics [1]. In comparison with conventional fusion welding processes, the power beam welding processes offer new perspectives in manufacturing due to the concentrated and reduced energy input. Depending on the power density on the surface, the welding takes place either in the conduction, in the transition or in the keyhole regime [2,3]. Deep-penetration keyhole welding processes are generally performed with a high-power focused electron or laser beam, having an excellent beam quality, achieving sufficient intensities on the surface of the workpiece. The electron beam welding, which is commonly applied in the manufacturing of powertrain components and work pieces having large wall thicknesses, exhibits several advantages over the laser beam processes, such as a higher quality and increased power of the beam, better inner

weld seam quality as well as deeper penetration [4]. Furthermore, the process is normally carried out in high vacuum, which prevents the material from oxidation, leading to a cleaner welding process. However, due to the significant disadvantages (e.g., higher machine and operating costs, generated X-ray during welding and sensibility on external magnetic field), the manufacturers tend to replace such systems with solutions based on novel high-brilliance solid-state laser sources [5]. These are characterized by a small spot size and a high beam quality, which generally provide the possibility of more precise manufacturing. In contrast to welding with CO₂ gas laser sources, the fiber lasers offer the possibility of an enhanced beam guidance and therefore a high flexibility [6]. However, the smaller spot sizes require a zero gap and consequently, the increased quality of weld seam preparation, which is generally a machining process, such as turning or milling. Keeping a constant zero gap challenges the manufacturing, causing high machining costs. Very often, the needed zero weld gap cannot be guaranteed due to the given dimensional and form tolerances of the part. Therefore, a multi-spot beam, a beam oscillation or a defocused beam should be applied in order to improve the gap bridging ability. However, due to the excellent beam quality and thus, very small beam divergence, the possibilities of the defocusing are limited, since it does not cause a huge increase of the spot diameter, which would be necessary for improved gap bridging. Hence, a dynamic beam oscillation can be a promising approach. The results of Aalerink et al. [7] show that using filler wire with single-spot or twin-spot largely increases the gap bridging ability. Without using multi-spot beam or filler wire, the maximum allowable gap width is 0.2 mm in case of welding of aluminum alloys. Schultz et al. [8] have conducted experiments to improve the gap bridging ability in laser beam welding of thin aluminum sheets. It has been worked out that a beam oscillation and the application of filler wire help to provide a complete fusion of the weld edges. Fixemer et al. have investigated the seam guided laser remote welding with automated gap bridging for welding of thin aluminum alloys and deep-drawing steel [9], focusing on overlap joints commonly applied in the automotive industry. Based on an integrated process model, the beam oscillation parameters were varied depending on the beam parameters and the gap size acquired with a laser triangulation feature. Using an adaptive beam oscillation, a vertical bridging of gap sizes up to 50% of the sheet thickness was achieved. Franciosa et al. have been dealing with a closed-loop gap bridging control at overlap welding of aluminum [10]. During their experimental work, a model has been developed for selecting appropriate welding process parameters such as beam oscillation to control the weld pool and improve the gap bridging possibility. It has been reported that the model gives a good approximation about the process behavior and makes possible the selection of feasible parameters. Another problematic issue of the solid-state laser is the fact that the keyhole mode welding often entails a high amount of spatter, which is in several applications, such as gearbox manufacturing, not acceptable [11]. In studies performed in recent years, it has been shown that through reduction of the ambient pressure, the process boundaries can be extended and the spatter formation can be reduced. Börner et al. [12] were focusing on the spatter formation and weld seam quality in laser-beam welding with solid-state laser at reduced ambient pressure. It has been shown that the penetration depth increases with the decrease of the ambient pressure, reaching a saturation at 100 mbar, especially in case of welding speeds below 3 m/min. At higher welding speeds, no influence of the ambient pressure was observed. Furthermore, the reduction of the ambient pressure leads to a minimized spatter formation due to the reduced friction between the metal vapor and the liquid phase. In addition, since the ambient pressure essentially determines the formation of the weld pool and vapor cavity, a more stable keyhole and thus, a reliable welding can be achieved even with lower vapor pressures and therefore, with reduced energy input. Arata et al. [13] have conducted experiments in a high-power CO₂ laser process under vacuum conditions in order to describe the behavior of laser plasma, the weld pool and the keyhole. It has been shown that the laser plasma appearing at keyhole welding was almost completely suppressed through the reduction of the ambient pressure. As the plasma does not longer shield the laser light, the absorption in the keyhole and thus the penetration increase, especially at lower welding speeds. According to Reisgen et al. [14], the process stability of the laser beam welding of copper at welding speed levels below

2 m/min is increased by a reduction of the ambient pressure to the range of 0.1 mbar. As main reasons, the reduced boiling point of the material, the eased formation of the vapor capillary as well as the suppressed metal vapor plume are assumed. These phenomena are also beneficial when welding low and unalloyed carbon steels as well as fine grained steels [15,16]. The research of Abe et al. [17] deals with the welding of X5CrNi18-10 (1.4301) stainless steel and AlMg2.5(B) (3.3523), using a high-power solid-state laser and reduced ambient pressure. In the case of stainless steel, 0.1 mbar ambient pressure leads to the highest penetration depth, causing a vase-form weld seam. In contrast to that, the highest penetration in the aluminum specimen was observed at 10 mbar, without a vase-formed weld geometry. Katayama et al. [18] reported about low amount of spatter and narrow weld seams, if reduced ambient pressure is used. It has also been found that humping may occur below 1 mbar; however, it can be suppressed with appropriate defocusing. Jiang et al. have investigated the processing window for full penetration laser welding of thick high strength steel under atmospheric and sub-atmospheric pressure conditions [19]. Using reduced ambient pressure, the processing window to achieve a full penetration weld was widened. At decreased ambient pressure, a parallel weld seam shape was obtained, in contrast to the nail-head shape appearing when using atmospheric pressure. Under 10 hPa, no further change of the weld geometry was observed. Peng et al. also investigated the weld formation and mechanical properties of solid-state laser welded aluminum alloys using subatmospheric pressures [20]. Below 1 hPa, large penetration depth and high process stability were achieved, combined with a significant reduction of the plasma plume. With decreasing pressure, a more uniform microstructure was observed. Furthermore, the average hardness and tensile strength have been increased, attributed to the inhibited porosity defects, the more uniform grain size distribution and the decreased burning loss of alloying elements. Based on the research findings, it can be stated that laser welding at reduced ambient pressures is generally beneficial due to the increased penetration depth and lack of spatter. Using the benefits of the vacuum combined with the high focusing ability of the laser beam, the process efficiency can be increased due to the possibility of using higher welding speeds or lower powers [21]. However, since the weld pool dynamic and melting point of a metal are affected by the vacuum, an altered gap bridging ability is to be expected compared to atmospheric conditions. Hence, the gap bridging ability shall be investigated at different welding speeds, gap sizes and ambient pressures. It can be assumed that with reduced ambient pressure and applying dynamic beam oscillation, an effective welding process with a low amount of spatter and good gap bridging ability can be achieved.

2. Materials and Methods

Considering applications in power train manufacturing, the investigations on gap bridging capability and beam oscillation were carried out using case hardening steel 1.7131 (16MnCr5) at an unhardened stage. The chemical composition is given in Table 1. Full penetration welds were performed as bead on plate welds as well as butt joints with different gap sizes using a plate thickness of 2 mm.

Table 1. Nominal composition of the case hardening steel 1.7131.

Chemical Composition (wt %) ¹						
Fe	C	Si	Mn	P	S	Cr
Bal.	0.14–0.19	<0.40	1.00–1.30	<0.025	<0.035	0.80–1.10

¹ according to manufacturer specifications.

The sample dimensions used in the welding trials are given in Figure 1. Prior to sample preparation, the sample surface was ground, whereas the weld joint surface was milled. To investigate the gap bridging capabilities a pre-set gap was adjusted using metal spacers (gauge tape). The samples were then tack-welded at the front sides using TIG-welding. In order to maintain constant gap sizes during welding, an additional spacer was positioned at the center of the weld length. After sample preparation, the gap was measured and evaluated using an optical microscope, ensuring that the pre-set gap size was

within the 10% limit in relation to the nominal gap size. Following a visual examination of the resulting weld seams according to ISO 13919-1, samples were taken at one third of the weld seam length for metallographic analysis. The samples were polished and etched using Nital etchant. A metallographic analysis was performed using an incident light microscope (Leica DM4000M, Leica Microsystems GmbH, Wetzlar, Germany). Based on the cross sections, the weld seam geometry was evaluated using *Imagic* image analysis (Imagic Bildverarbeitung AG, Glattbrugg, Switzerland) regarding geometric criteria (undercuts, shrinkage grooves, incompletely filled grooves, excess weld metal) according to ISO 13919-1. As a decisive factor for the gap bridging ability, the missing cross-section of the bond was determined as the difference between the sheet thickness s and the minimal cross-section s' (see Figure 1 (right)). The missing cross section $(s-s')$ /mm weld length is determined in weld seam length direction and expressed in mm^2/mm length.

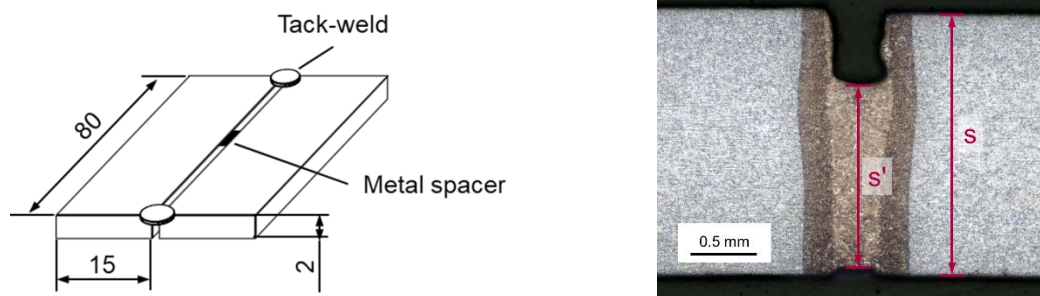


Figure 1. Sample dimensions for the welding trials (left) and evaluation of the cross-section (right).

The welding trials were performed at a custom-built vacuum chamber. Figure 2 shows an overview of the vacuum chamber as well as the schematic design of the beam guidance. The chamber with a volume of approx. 0.25 m^3 contains a XY-cross table for weld specimen movement. The maximum travel speed of the XY-cross table is 10 m/min with an axis acceleration of 0.5 m/s^2 . With the stated setup a positioning accuracy of $\pm 0.1 \text{ mm}$ at a repeatability of 0.02 mm can be achieved. The laser beam is fed into the chamber via two coupling glasses. As shown in Figure 2 (right), the first protection glass is sealing off the ambient pressure, whereas the second protection glass is inserted between the first one and the weld specimen in order to protect the main coupling glass from weld fumes and spatter. Furthermore, the beam path between the second glass and the specimen is rinsed with nitrogen to prevent welding fumes from condensing at the glass. The vacuum system connected with the chamber consists of a multiple stage Roots pump with a discharge pressure of 0.01 hPa. As beam source a diode-pumped Yb:YAG disc laser (TruDisc 6002 by TRUMPF, Ditzingen, Germany) with a maximum output power of 6 kW was used. The beam guidance between laser source and processing optics (TRUMPF PFO-3D, Ditzingen, Germany) was implemented using an optical fiber with a core diameter of $200 \mu\text{m}$. Based on the optical configuration the spot diameter of the laser beam at the focus position was $375 \mu\text{m}$. All welding trials were performed in focal position. In order to obtain comparable results, laser beam welding at atmospheric and reduced ambient pressure was performed without the use of shielding gas at ambient atmosphere. Unless stated otherwise, welding trials at reduced ambient pressure were performed at 10 hPa. To provide further information on weld spatter behavior, weld spatter formation was qualitatively determined through process monitoring using videography (Nikon D800, Tokyo, Japan).

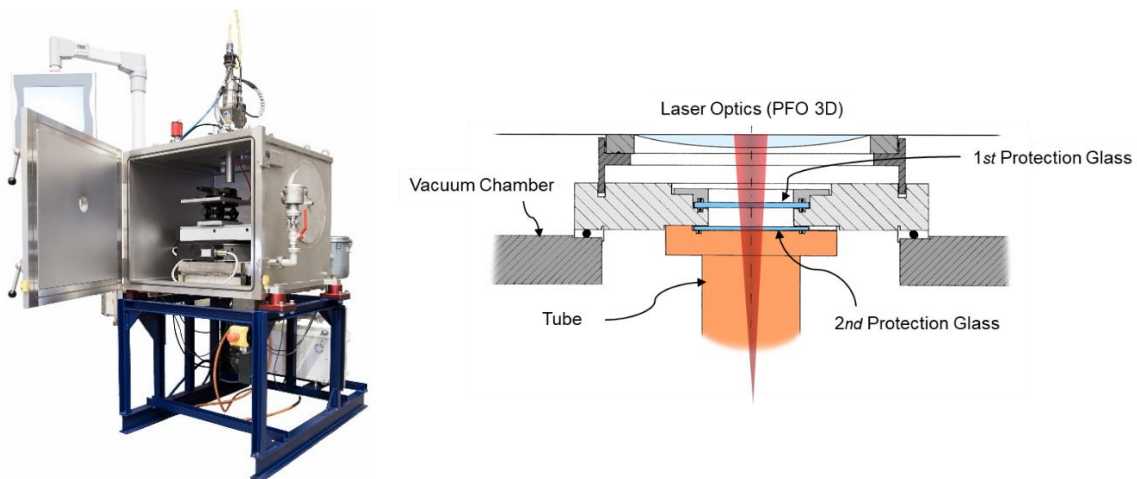


Figure 2. Experimental setup for laser welding at reduced ambient pressure (**left**) and schematic beam guidance (**right**).

In order to describe the effects of a reduced ambient pressure and beam oscillation on the gap bridging ability during laser beam welding, the experiments were subdivided in three stages:

A first set of experiments was performed to determine the influence of a reduced ambient pressure on the gap bridging ability without applying beam oscillation. Therefore, welding trials at different welding speeds of 0.5–5.0 m/min were performed at ambient pressure as well as at 10 hPa under variation of the preset gap size (zero gap up to 0.3 mm) using a full factorial design of experiments.

Secondly, different beam oscillation patterns were investigated at both atmospheric and reduced ambient pressure aiming to increase the gap bridging abilities. The purpose of the experiments was to increase the melt pool volume and simultaneously ensure a homogeneous filling of the gap. Therefore, a basic evaluation of different oscillation patterns was conducted to determine the effect of oscillation parameters on the weld outcome. Compared to conventional laser beam welding, additional parameters such as oscillation pattern, amplitude and frequency can affect the welding outcome while welding with beam oscillation and therefore have to be considered for process settings. Based on common oscillation patterns used during electron beam welding, four different patterns were considered for further investigation (line, circle, eight frame (crosswise) and eight frame (lengthwise)). In this set of experiments, the welding parameters laser power and ambient pressure as well as the oscillation parameters amplitude and frequency were varied at a set welding speed of $v_s = 1.0$ m/min and the resulting welds were evaluated regarding weld seam quality and spatter formation. The oscillation frequency was varied at three stages. Thereby, a minimal frequency was set at the value where the beam displacement during one period equals the beam diameter (25–45 Hz, depending on the oscillation pattern). Additionally, the maximum possible frequency based on the deflection rate of the scanner optics (210–520 Hz, depending on the oscillation pattern) and a medium frequency (mean value between min. and max. frequency) were evaluated. The laser power was adjusted for each parameter setting to ensure a full penetration weld.

Based on the optimized parameter settings, a case-study approach was adopted to determine the gap bridging abilities using beam oscillation. Therefore, welding trials using the previously regarded oscillation patterns were performed under variation of the gap size and ambient pressure at a third stage.

3. Results

3.1. Gap Bridging at Reduced Ambient Pressure

During the first sequence of welding experiments, the laser power was adjusted in order to reach a full penetration and obtain a good weld geometry at corresponding welding speed and ambient

pressure. Table 2 provides an overview of the applied welding speed, laser power as well as the energy input per unit length.

Table 2. Laser welding parameters selected for the investigation of gap bridging ability.

Welding Speed [m/min]	Atm.		10 hPa	
	Laser Power [W]	Energy per Unit Length [J/mm]	Laser Power [W]	Energy per Unit Length [J/mm]
0.5	700	84.0	550	66.0
1.0	950	57.0	700	42.0
2.0	1375	41.3	1000	30.0
5.0	2200	26.4	2150	25.8

Based on the metallographic cross sections as well as the process monitoring, the gap bridging ability of the process was analyzed at different welding speeds and ambient pressures. During these tests, no beam oscillation was applied. The investigations have revealed that gap sizes up to 0.1 mm do not affect the process stability, causing neither excessive root penetration nor significant loss in the joint cross section independent from the applied ambient pressure. Figure 3 shows the macrographs of the welded joints, which were prepared with 0.2 mm gap and welded at atmospheric and reduced ambient pressure, applying different welding speeds. The welding process exhibits a lower sensitivity on the gap size, if atmospheric ambient pressure is used. At lower welding speeds (up to 1 m/min), a complete fusion without any external weld imperfection can be achieved. At elevated welding speeds, weld seams with a good integrity have been realized, although partial incomplete fusion and consequently small loss in the joint cross section were observed. It can be clearly seen in the figure that the gap bridging ability significantly decreases at reduced ambient pressure. When applying reduced ambient pressure at low welding speed, a distinct weld root dropout can be observed. In contrast, welding speeds higher than 0.5 m/min result in a severe loss in the joint cross section.

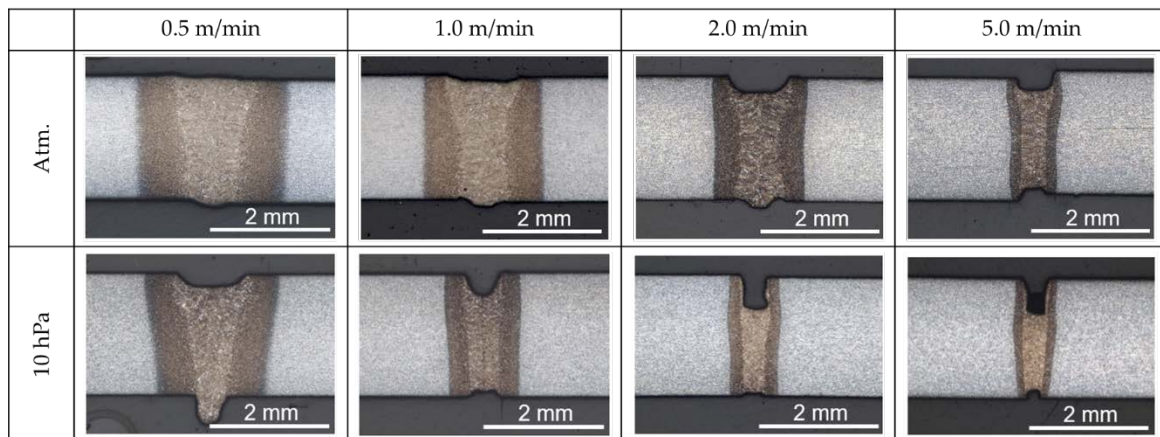


Figure 3. Macrographs of the specimens prepared with 0.2 mm gap, performed with different welding speeds at atmospheric pressure and 10 hPa.

Further increase of the gap size led to a rapid decrease of the process stability under atmospheric pressure, enabling welding only using a travel speed lower than 1 m/min. The reduction of the ambient pressure led to an incomplete fusion of the groove faces and therefore to an excessive loss or even a complete missing of the joint cross section. Figure 4 reveals the missing cross section of the joints in dependence of the welding speed and the gap sizes at atmospheric and reduced ambient pressure. What stands out in this figure is the phenomenal growth of the missing cross section with the increase of the gap size at atmospheric as well as reduced ambient pressure. Furthermore, the increase of welding speed results in an enlarged missing section under atmospheric pressure conditions. At reduced

ambient pressure and gap sizes up to 0.1 mm, the missing cross-section can be decreased through increase of travel speed.

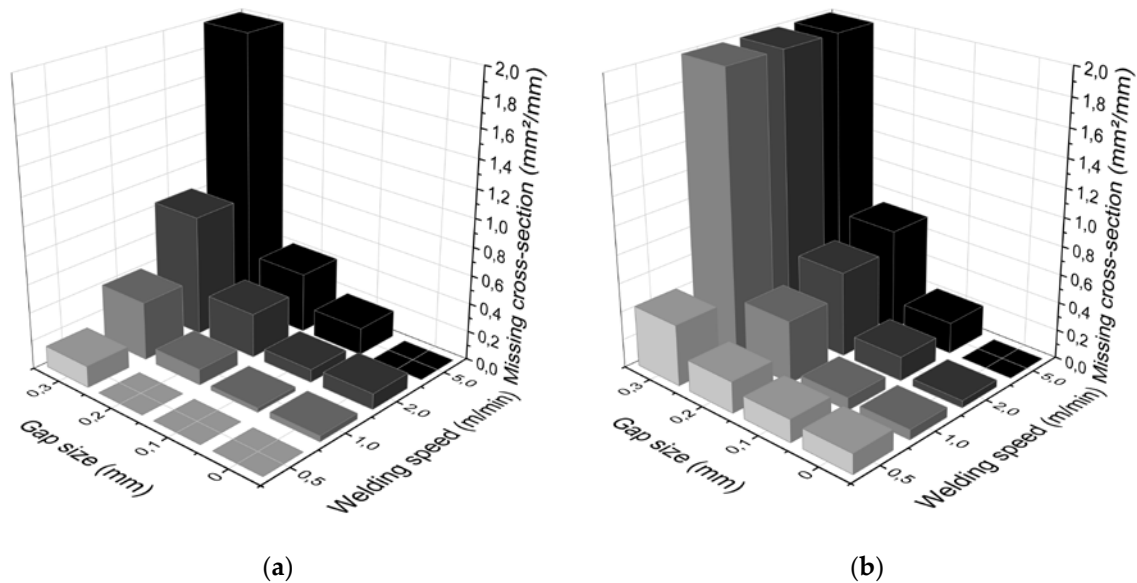


Figure 4. Missing cross-section per mm weld seam length depending on welding speed and gap size for welding at atmospheric pressure (a) and 10 hPa (b).

In addition, the spatter and metal vapor plume formation were observed at all welding tests. The reduction of the ambient pressure led to a significant decrease of the spatter formation and suppression to the metal vapor plume, as is shown in Figure 5 and was stated in the previous studies [12,13,18,20].

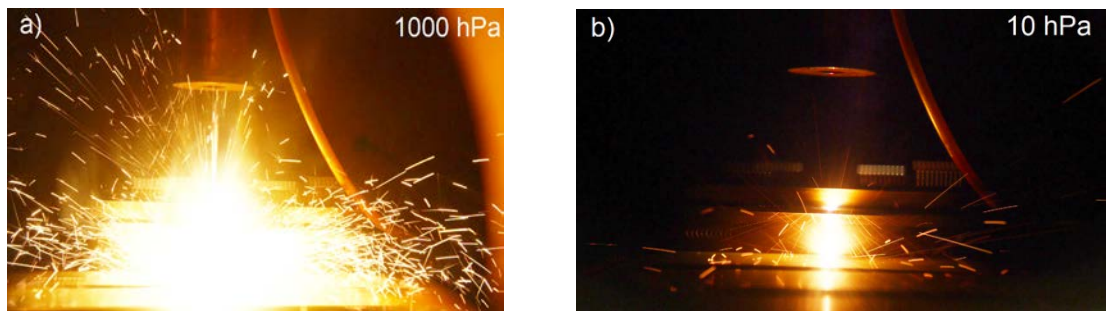


Figure 5. Spatter and metal vapor plume in the case of 0.2 mm gap, performed with 5 m/min welding speed and different ambient pressure ((a): 1000 hPa and (b): 10 hPa).

3.2. Gap Bridging Using Beam Oscillation in Combination with Reduced Ambient Pressure

3.2.1. Basic Evaluation of Oscillation Patterns

In the case of welding with beam oscillation, scanner optics was used to perform the beam pattern movement, which was superposed with the cross-table movement, resulting in the trajectory of the welding path. As provided in Figure 6, the resulting trajectories of the actual beam paths show major differences in symmetry and motion dynamics. Therefore, different effects on weld seam formation as well as processing behavior can be expected.

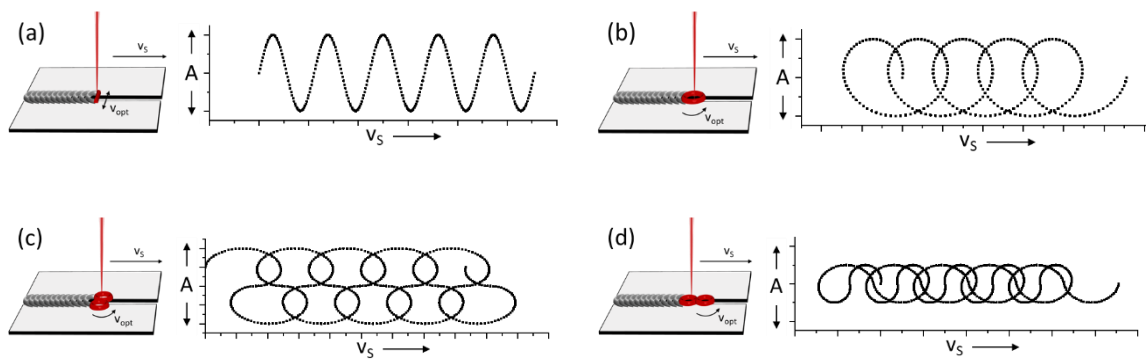


Figure 6. Schematic trajectory of the welding path for oscillation patterns: line (a), circle (b), eight frame crosswise (c) and eight frame lengthwise (d).

Based on the parameter evaluation of different oscillation patterns the following key findings can be derived:

- While using a beam oscillation, the most frequent weld seam irregularities are notches and lateral spill of the melt pool.
- At atmospheric pressure, the weld seam formation is in most parts independent of the oscillation frequency. Significant differences depending on the oscillation frequency could be observed using a circle pattern. Thereby, high frequencies led to an asymmetrical cross-section of the weld seam.
- At reduced ambient pressure, the formation of weld seam irregularities is largely dependent on the oscillation frequency. However, no universal criteria on the connection between parameter settings and irregularities could be found.
- Based on the results from process monitoring, the weld spatter formation is generally diminished at reduced ambient pressure.

The results of the basic process evaluation of oscillation patterns indicate that the amplitude as well as the oscillation pattern affect the size of the fusion zone. Furthermore, a change towards higher melt viscosity during laser beam welding at reduced ambient pressure is described in the literature [12,15]. Therefore it is assumed, that the change in melt viscosity also changes the specific damping of the melt pool, causing lateral spills of the melt pool at specific excitation frequencies of the beam oscillation. To complement these findings, the detailed analysis of eigenfrequencies depending on the melt pool size should therefore state the scope of further research.

For the selection of suitable process settings, the data suggest that optimized parameters have to be determined separately according to the oscillation pattern. Based on the results, the optimized parameter settings for the investigation of gap bridging ability are summarized in Table 3.

Table 3. Laser welding parameters selected for the investigation of gap bridging ability using beam oscillation (vs. = 1.0 m/min).

Pattern	Amplitude ¹ [mm]	Frequency [Hz]	Laser Power [W]	Energy per Unit Length [J/mm]
Line	2.0	45	2000	120
Circle	2.0	25	1400	84
Eight frame (crosswise)	1.0	235	1100	66
Eight frame (lengthwise)	1.0	45	1440	84

¹ transversely to welding direction.

In zero gap configuration, weld seams without geometrical irregularities (Group B according to ISO 13919-1) could be achieved through the adjustment of oscillation frequency and laser power

depending on the applied oscillation pattern. Figure 7 shows the cross-sections of laser beam welds obtained using different oscillation patterns. Compared to non-oscillated welding trails, the weld seam width could be generally increased using beam oscillation. With the exception of the eight frame (crosswise) pattern, the weld seams show parallel joint faces. Further, the eight frame (crosswise) pattern led to a narrower weld seam geometry, which can be attributed to a concentrated energy input in the middle of the weld seam due to the trajectory of the weld path. What stands out from the welding trials at reduced ambient pressure is that the weld seams were generally slightly narrower and more defined compared to welding at atmospheric pressure. In case of the circle pattern, an asymmetrical formation of the weld bead could be observed. Therefore, it is assumed, that welding at reduced ambient pressure is more sensitive to the energy distribution during welding.

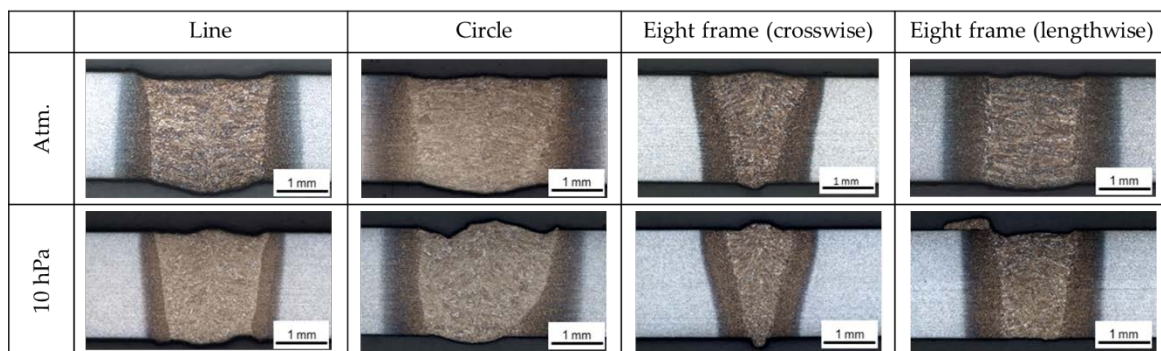


Figure 7. Resulting weld seam geometry using different laser oscillation patterns at atmospheric pressure and 10 hPa.

The spatter formation during welding was observed using video imaging. In order to ensure comparability, single frames from one second of the welding process were extracted and superposed. The superposed images are provided in Figure 8. During welding at atmospheric pressure, a bright radiation of the vapor plume as well as an intense formation of weld spatters are visible on the top and bottom side of the weld specimen. At reduced ambient pressure (10 hPa), the vapor plume and the spatter formation on the top side of the specimen are visible weakened, whereas the bottom side of the specimen still exhibits a distinct weld spatter formation. Generally, at reduced ambient pressure, the reduction of weld spatter formation was found to be lower while welding with beam oscillation compared to stationary laser beam.

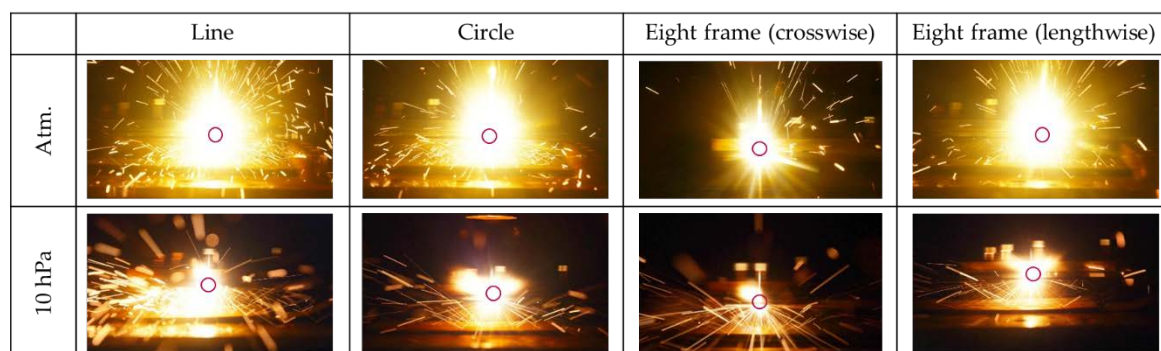


Figure 8. Spatter formation and metal vapour plume using different laser oscillation patterns at atmospheric pressure and 10 hPa; weld location marked with red circle.

3.2.2. Investigation of Gap Bridging Ability

In order to identify the gap bridging ability using laser beam welding with different beam oscillation patterns, samples with preset gaps of 0.2 mm and 0.4 mm were welded at both atmospheric

and reduced ambient pressure and analyzed. From visual inspection of the weld seam top and root surface, a significant decrease in weld quality could be detected for specimens welded using the circle pattern at reduced ambient pressure with a gap present. Accordingly, these samples were not further evaluated. By contrast, samples welded at atmospheric pressure using the circle pattern showed no significant loss in quality. Figures 9 and 10 provide an overview of micrographs of the welded joints prepared with a 0.2 mm and 0.4 mm gap. It can be seen from the micrographs that all samples showed more or less distinct undercuts of the upper weld bead due to the size of the present gap. Thereby, the undercut is most pronounced for the eight frame (crosswise) pattern. Compared to other oscillation patterns, less metal is molten at the joint faces and therefore only a limited amount of molten metal is available to fill the gap, resulting in a significant reduction of the load-bearing cross-section. In general, a decreased gap bridging ability was found for welding at reduced ambient pressure (10 hPa). These results are likely to be related to the formation of narrower weld seam geometries observed during welding at reduced ambient pressure.

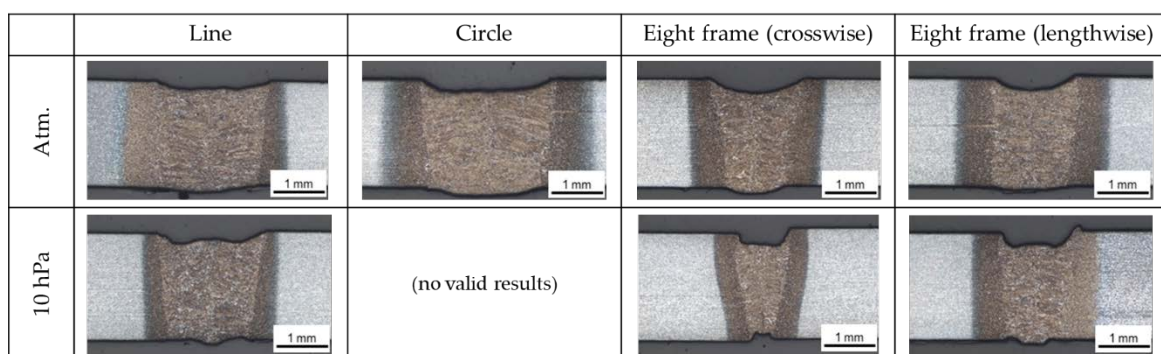


Figure 9. Macrographs of specimens prepared with a 0.2 mm gap, welded using different oscillation patterns at atmospheric pressure and 10 hPa.

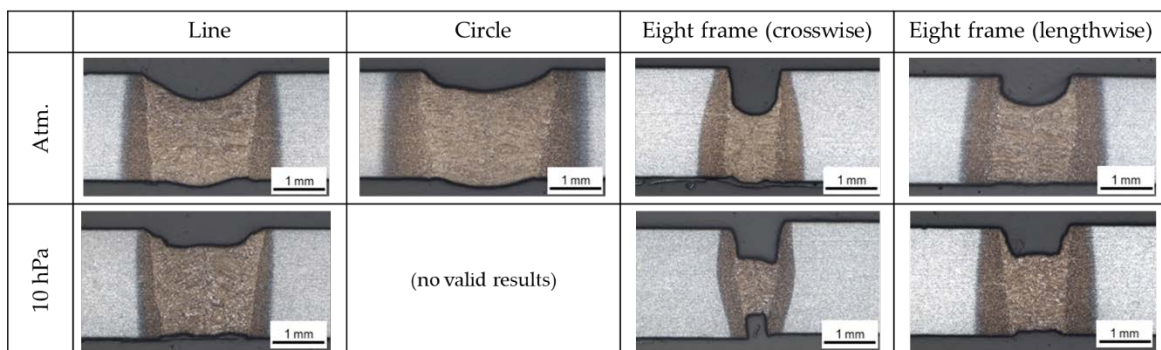


Figure 10. Macrographs of specimens prepared with a 0.4 mm gap, welded using different oscillation patterns at atmospheric pressure and 10 hPa.

According to ISO 13919-1 all evaluable samples welded with a gap of 0.2 mm matched the geometric criteria (undercuts, shrinkage grooves, incompletely filled grooves, excess weld metal) for level C or level B in case of line pattern at atmospheric pressure. With a gap of 0.4 mm, the quality of the weld was found to be lowered to level D or outside of the specification for weldments using the eight frame (crosswise) pattern. Compared to welding with a non-oscillated laser beam (see Figure 3), an improvement in gap bridging ability could be observed for welding with beam oscillation due to an increased seam width at both atmospheric and reduced ambient pressure.

A key factor regarding the component integrity is the load-bearing cross-section. Therefore, samples were analyzed regarding the missing cross-section due to undercut, incompletely filled grooves and root relapse. A quantitative overview of the missing cross-section depending on the gap size during welding is given in Figure 11. For welding at atmospheric pressure, the chart illustrates

that the cross-section was reduced by an average of $0.2 \text{ mm}^2/\text{mm}$ when the gap was 0.2 mm . With a gap of 0.4 mm the missing cross-section was increased to approx. $0.5 \text{ mm}^2/\text{mm}$ and up to $0.9 \text{ mm}^2/\text{mm}$ for the eight frame (crosswise) pattern. At reduced ambient pressure, both eight frames showed an increased missing cross-section while the line pattern could match the values at ambient pressure.

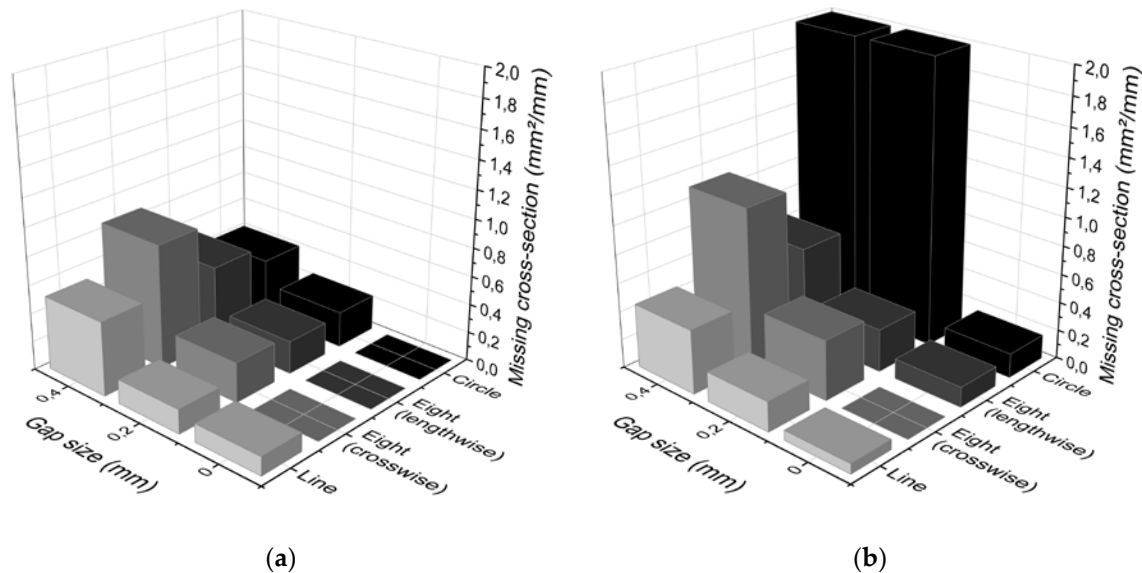


Figure 11. Missing cross-section per mm weld seam length depending on welding speed and gap size for welding at atmospheric pressure (a) and 10 hPa (b).

In summary, the results show that different oscillation patterns in combination with different ambient pressure can lead to varying gap bridging abilities. In this study, oscillation patterns, which resulted in narrower weld seam geometries (eight frame) provided lower gap bridging ability compared to line or circle pattern. Furthermore, the asymmetrical energy distribution using a circle oscillation pattern was found to result in an unstable welding process at reduced ambient pressure and is therefore not unrestricted recommendable.

4. Conclusions

Laser beam welding with solid-state laser sources offers numerous advantages for automotive applications, including low energy input, high processing rates and a high level of process availability thorough laser processing networks. Due to decreasing sizes of the focal spot, modern laser beam sources place high requirements on weld seam preparation, allowing only minimal gaps. Likewise, a minimized weld spatter formation is required in many applications. The aim of the present research was to assess the influence of both a reduced ambient pressure in the process environment as well as beam oscillation on the gap bridging ability during laser beam welding. Based on the welding experiments and the weld quality analysis, the following conclusions are derived:

- During single spot laser beam welding without beam oscillation, using the applied optical configuration, gaps exceeding 0.1 mm can lead to significant loss in weld quality.
- A reduction in welding speed has positive impact on the gap bridging ability at the considered range of $v_s = 0.5\text{--}5.0 \text{ m/min}$.
- While welding at reduced ambient pressure, a reduced gap bridging ability was observed due to a more narrow weld seam geometry. However, the weld spatter formation was significantly improved.
- Beam oscillation can be applied to increase the weld width and enlarge the melt pool volume to ensure a homogeneous filling of the gap. The results at reduced ambient pressure suggest a

heighten sensitivity for a change of process parameters (especially oscillation frequency) and therefore a smaller processing window.

- Using beam oscillation, gaps with 0.2 mm could reliably be welded. Gaps with 0.4 mm showed sufficient quality.

Building on the reported results, further research should include mechanical-technological examinations to identify the effects of gap induced weld defects on the mechanical properties during static and dynamic loading. Although no internal welding defects could be detected by means of metallographic cross sections, non-destructive testing should be considered to verify these results. Furthermore, high-speed process monitoring of the melt pool behavior during welding with beam oscillation is suggested to establishing results on how the oscillation frequency affects the occurrence of welding defects.

Author Contributions: Conceptualization, M.K. and J.H.; Data curation, J.H.; Formal analysis, A.K.; Funding acquisition, K.D.; Investigation, M.K. and A.K.; Methodology, M.K. and A.K.; Project administration, J.H.; Resources, K.D.; Supervision, J.H. and K.D.; Validation, T.T. and J.H.; Visualization, M.K., T.T. and A.K.; Writing—original draft, M.K. and T.T.; Writing—review and editing, J.H. All authors have read and agreed to the published version of the manuscript.

Funding: The IGF-research project 19.732N of the Research Association FOSTA Forschungsvereinigung Stahlanwendung e.V. is funded by the AiF within the program to promote Joint Industrial Research (IGF) by the Federal Ministry for Economic Affairs and Energy, following a decision by the German Bundestag.

Acknowledgments: The authors would like to express their appreciation for the technical support provided by TRUMPF GmbH + Co. KG and the support with consumables by Salzgitter AG.

Conflicts of Interest: The authors declare no conflict of interest. The funders had no role in the design of the study; in the collection, analyses, or interpretation of data; in the writing of the manuscript, or in the decision to publish the results.

References

1. Havrilla, D.; Holzer, M. High power disk lasers: Advances and applications. In Proceedings of the SPIE LASE, Solid State Lasers XX: Technology and Devices, San Francisco, CA, USA, 21–26 January 2011; Volume 7912. [CrossRef]
2. Kannatey-Asibu, E., Jr. *Principles of Laser Materials Processing Laser Welding*; John Wiley & Sons, Inc.: Hoboken, NJ, USA, 2008. [CrossRef]
3. Svenungsson, J.; Choquet, I.; Kaplan, A. Laser Welding Process—A Review of Keyhole Welding Modelling. *Phys. Procedia* **2015**, *78*, 182–191. [CrossRef]
4. Reisgen, U.; Olschok, S.; Jakobs, S. A comparison of electron beam welding with laser beam welding in vacuum. DVS-Berichte. In Proceedings of the 2nd International Electron Beam Welding Conference, Aachen, Germany, 26–30 March 2012; Volume 285, pp. 119–127.
5. Reisgen, U.; Olschok, S.; Holtum, W.N.; Jakobs, S. Laser beam welding in mobile vacuum. In Proceedings of the Lasers in Manufacturing, Munich, Germany, 26–29 June 2017. Available online: <https://publications.rwth-aachen.de/record/692293> (accessed on 26 February 2019).
6. Webb, C.E.; Jones, J.D.C. *Handbook of Laser Technology and Applications Volume III: Applications*; Institute of Physics: Bristol, UK, 2004.
7. Aalderink, B.J.; Pathiraj, B.R.G.K.M.; Aarts, R.G.K.M. Seam gap bridging of laser based processes for the welding of aluminium sheets for industrial applications. *Int. J. Adv. Manuf. Technol.* **2010**, *48*, 143–154. [CrossRef]
8. Schultz, V.; Seefeld, T.; Vollertsen, F. Gap Bridging Ability in Laser Beam Welding of Thin Aluminum Sheets. *Phys. Procedia* **2014**, *56*, 545–553. [CrossRef]
9. Fixemer, P.; Albert, F.; Sievi, P.; Graham, T. Seam Guided Laser Remote Welding with Automated Gap Bridging. *Laser Tech. J.* **2015**, *21*, 38–41. [CrossRef]
10. Franciosa, P.; Serino, A.; Al Botros, R.; Ceglarek, D. Closed-loop gap bridging control for remote laser welding of aluminum components based on first principle energy and mass balance. *J. Laser Appl.* **2019**, *31*. [CrossRef]
11. Rominger, V. High-performance laser welding: A comparison of CO₂ lasers and high-brilliance solid-state lasers. *Laser Tech. J.* **2011**, *8*, 32–35. [CrossRef]

12. Börner, C.; Dilger, K.; Rominger, V.; Harrer, T.; Krüssel, T.; Löwer, T. Influence of ambient pressure on spattering and weld seam quality in laser beam welding with the solid-state laser. In Proceedings of the International Congress on Applications of Lasers & Electro-Optics, Orlando, FL, USA, 23–27 October 2011; pp. 621–629. [[CrossRef](#)]
13. Arata, Y.; Abe, N.; Oda, T.; Tsujii, N. Fundamental phenomena during vacuum laser welding. In Proceedings of the International Congress on Applications of Lasers & Electro-Optics, Boston, MA, USA, 12–15 November 1984; pp. 1–7. [[CrossRef](#)]
14. Reisgen, U.; Olschok, S.; Jakobs, S.; Turner, C. Sound Welding of Copper: Laser Beam Welding in Vacuum. *Phys. Procedia* **2016**, *83*, 447–454. [[CrossRef](#)]
15. Reisgen, U.; Olschok, S.; Jakobs, S. Laser beam welding under vacuum of a fine-grained steel. In Proceedings of the International Congress on Applications of Lasers & Electro-Optics, San Diego, CA, USA, 19–23 October 2014; pp. 933–940. [[CrossRef](#)]
16. Reisgen, U.; Olschok, S.; Jakobs, S. Laser beam welding in vacuum of thick plate structural steel. In Proceedings of the International Congress on Applications of Lasers & Electro-Optics, Miami, FL, USA, 6–10 October 2013; pp. 341–350. [[CrossRef](#)]
17. Abe, Y.; Mizutani, M.; Kawahito, Y.; Katayama, S. Deep penetration welding with high power laser under vacuum. In Proceedings of the International Congress on Applications of Lasers & Electro-Optics, Anaheim, CA, USA, 27–30 September 2010; pp. 648–653. [[CrossRef](#)]
18. Katayama, S.; Abe, Y.; Mizutani, M.; Kawahito, Y. Deep penetration welding with high power disk lasers in low vacuum. In Proceedings of the International Congress on Applications of Lasers & Electro-Optics, Orlando, FL, USA, 23–27 October 2011; pp. 669–678. [[CrossRef](#)]
19. Jiang, M.; Tao, W.; Chen, Y.; Li, F. Comparison of processing window in full penetration laser welding of thick high-strength steel under atmosphere and sub-atmosphere. *Opt. Laser Technol.* **2019**, *109*, 449–455. [[CrossRef](#)]
20. Peng, G.; Li, L.; Wang, J.; Xia, H.; Meng, S.; Gong, J. Effect of subatmospheric pressures on weld formation and mechanical properties during disk laser welding of 5A06 aluminium alloy. *J. Mater. Process. Technol.* **2020**, *277*, 116457. [[CrossRef](#)]
21. Bergmann, J.P.; Patschger, A.; Bastick, A. Enhancing Process Efficiency due to high Focusing with high Brightness Lasers—Applicability and constraints. *Phys. Procedia* **2011**, *12*, 66–74. [[CrossRef](#)]



© 2020 by the authors. Licensee MDPI, Basel, Switzerland. This article is an open access article distributed under the terms and conditions of the Creative Commons Attribution (CC BY) license (<http://creativecommons.org/licenses/by/4.0/>).